Hindawi Publishing Corporation
Journal of Catalysts
Volume 2014, Article ID 869472, 8 pages
http://dx.doi.org/10.1155/2014/869472

Research Article

Preparation of Mesoporous SiO_2-Pillared Lamellar Titanoniobate Catalysts for Bioethanol Dehydration

Olivalter Pergentino,[1] Marina M. de Brito,[1] Heloysa M. C. Andrade,[1,2] and Artur J. S. Mascarenhas[1,2]

[1] *Laboratório de Catálise e Materiais, Departamento de Química Geral e Inorgânica, Instituto de Química, Universidade Federal da Bahia(UFBA), Rua Barão de Jeremoabo 147, Campus Universitário da Federação, 40170-280 Salvador, BA, Brazil*
[2] *Instituto Nacional de Ciência e Tecnologia em Energia e Ambiente(INCT-E&A), Universidade Federal da Bahia, 40170-115 Salvador, BA, Brazil*

Correspondence should be addressed to Artur J. S. Mascarenhas; artur@ufba.br

Received 24 October 2013; Revised 11 December 2013; Accepted 12 December 2013; Published 9 January 2014

Academic Editor: Raghunath V. Chaudhari

The lamellar perovskite $K_{0,8}Ti_{0,8}Nb_{1,2}O_5$ was prepared by solid state reaction, and its protonic form was used in a sequence of intercalation steps with n-butylamine, cetyltrimethylammonium bromide (CTABr), and tetraethyl orthosilicate (TEOS). After calcination, a high surface area, mesoporous SiO_2-pillared titanoniobate, was obtained. The samples were characterized by XRD, EDX, TG-DTG, N_2 adsorption isotherms, and NH_3-TPD. The pillarization procedure affected the textural properties, the amount, and strength distribution of acid sites. The influence of the pillarization procedure on the catalytic properties of the lamellar titanoniobates was investigated on ethanol dehydration. High ethanol conversions and ethylene yields (>90%) were obtained in the presence of the SiO_2-pillared titanoniobate catalyst, at 350–450°C.

1. Introduction

Since the last decades, the intercalation chemistry of lamellar materials has been used as a strategy either to modify or produce innovative materials designed for some special applications [1]. In this sense, clays, graphite, some halides or oxides of transition metals, phosphates, and sulfides have been investigated as host materials to produce semiconductors, sensors, electrodes, catalysts, photocatalysts, and so forth [2–7].

Potassium titanoniobate, $KTiNbO_5$, is a lamellar perovskite built up of edge sharing TiO_6^{8-} and NbO_6^{7-} octahedral forming strings that are connected by sharing corners to form a layered structure intercalated with alkaline cations (K^+), which compensate the negative charge in the interlayer space [8]. This material can be synthesized by solid state reaction, but some studies hve been published recently showing that $KTiNbO_5$ can be prepared by hydrothermal synthesis at lower temperatures with different particle sizes and morphologies, depending on the solvent used during the process [9].

Independently of the synthesis method, interlayer K^+ cations are exchangeable, allowing the intercalation of species of different sizes that result in a variety of composites of improved properties [8]. For example, substitution of K^+ by H^+ cations produces $HTiNbO_5$ that can be a strong Brönsted acid comparable to some zeolites [10]. In spite of this, the use of this protonic form as a heterogeneous acid catalyst is still limited by textural properties, such as low surface area and porosity [11]. Exfoliation of $KTiNbO_5$ or $HTiNbO_5$ has been investigated, but the resultant colloids are adequate only for photocatalytic purposes [12]; but for traditional heterogeneous acid-catalyzed processes it would be necessary to precipitate the exfoliated nanosheets, and the resulting materials usually do not reach the theoretical surface area expected for a fully separated nanosheets. Dias et al. [13] prepared an exfoliated $HTiNbO_5$ material by intercalating tetrabutylammonium cations and precipitated

the nanosheets using HNO_3 or MgO, and the resulting materials presented surface areas of 81 and 103 $m^2\,g^{-1}$, respectively. The exfoliated $HTiNbO_5$-MgO material has presented high xylose conversion (92%) and furfural yields (55%) after 4 h of reaction.

The improvement of the textural properties can be performed by pillarization of the layered precursor and some studies have been reported in the literature for $KTiNbO_5$ derived materials. For instance, Chen et al. [14] prepared a chromia-pillared titanoniobate by calcination of oligomeric Cr(III)-intercalated titanoniobate at 400°C. The resulting porous solid contained only acid sites and was proven to be a very active catalyst for the dehydration of propyl alcohol. Wang et al. [15] have obtained a silica-pillared titanoniobate by intercalation of $NH_2(CH_2)_3Si(OEt)_3$ and the inorganic material was used as catalyst support. In both cases, the surface areas of final products attained 122.4 $m^2\,g^{-1}$ and 132.3 $m^2\,g^{-1}$, respectively.

In order to improve the chemical and textural properties of SiO_2-pillared titanoniobates, Shangguan et al. [16] have intercalated progressively larger precursors into the interlayer space of $KTiNbO_5$. Thus, $HTiNbO_5$ was initially intercalated with n-hexylamine and then used as precursor for the intercalation of tetraethyl orthosilicate (TEOS). Nevertheless, the interlayer distance and the crystallinity of the resulting material decreased after calcinations to form the silica pillars.

A TiO_2-pillared $HTiNbO_5$ was prepared by Guo et al. [17] by exchanging titanium(IV) polycations species generated by acid hydrolysis of titanium(IV) isopropoxide in a n-decylamine preswelled $HTiNbO_5$, obtaining a material with a specific surface area of 89 $m^2\,g^{-1}$. This material has proven to be very active in the Beckman rearrangement of cyclohexanone oxime to ε-caprolactam.

Recently, Fan et al. [18] prepared a TiO_2-pillared $HTiNbO_5$ material by adding a monodisperse TiO_2 sol to a colloidal suspension of exfoliated $HTiNbO_5$ nanosheets. The material was coated with Pt and evaluated in the photocatalytic hydrogen evolution from water. The hybrid material gave a remarkable hydrogen evolution rate of 4735 $mmol\,h^{-1}\,g^{-1}$, which was partially due to the improved surface area of 171 $m^2\,g^{-1}$ observed for $TiO_2/HTiNbO_5$.

In the present work, the preparation and characterization of a high surface area SiO_2-pillared titanoniobate are described. The pillaring procedure consisted in a sequence of intercalation steps using progressively larger precursors to enlarge the interlayer space of the pristine $KTiNbO_5$, resulting in a uniform material of improved surface area and porosity. The properties of the prepared materials were also compared on the catalytic dehydration of sugar cane derived ethanol (bioethanol), which is now envisaged as a promising route for obtaining ethylene from a renewable source.

2. Material and Methods

2.1. Reagents and Synthesis Process. A perovskite type layered titanoniobate ($KTiNbO_5$, here called KTN) was synthetized by solid state reaction. Stoichiometric amounts of the reagents TiO_2 (Aldrich 99%) and $Nb_2O_5{\cdot}nH_2O$ (CBMM 76.3%) were mixed with 20% excess of K_2CO_3 (Anidrol 99%). This homogeneous mixture was heated in a muffle furnace at 1150°C for 24 h. The product was crushed, sieved, and then cation-exchanged with a 6 mol L^{-1} HNO_3 aqueous solution, at 60°C for 48 h, resulting in a protonic form ($HTiNbO_5$) that was used in a sequence of intercalation steps as follows.

Step 1. The protonic titanoniobate, $HTiNbO_5$ (or simply HTN), was washed with deionized water until pH = 7 and then refluxed in a solution of 10% n-butylamine in n-heptane (100 mL/g of precursor), at room temperature. After 7 days, the solids were vacuum-filtered and washed with heptane to remove the excess of n-butylamine and air-dried at room temperature.

Step 2. The resulting product of Step 1 was stirred in an aqueous solution of cetyltrimethylammonium bromide, CTABr, (10%) at room temperature (28°C) for 48 h. The resulting intercalation product, CTATN, was thoroughly washed with distilled water to remove the surfactant excess and dried in a desiccator at room temperature.

Step 3. Silica-pillared titanoniobate (SiO_2TN) was prepared by adding the precursor powder prepared in Step 2 to an excess of tetraethyl orthosilicate, TEOS (1 g precursor/38 g TEOS). The dispersion was stirred in a nitrogen inert atmosphere for 25 h at 90°C, filtered, and then overnight air-dried at room temperature. The solid product was further treated in excess water (1 g precursor : 10 g water) for 12 h at 100°C to hydrolyze the silica precursor in the lamellar structure, filtered, and heated (2°C min^{-1}) in an N_2 flow for 3 h at 450°C and then at 540°C in an air flow, 6 h.

2.2. Material Characterizations. The powder products were analyzed by X-ray diffraction on a Shimadzu XRD-6000, operating with CuK_α (40 kV and 30 mA). The chemical composition of the samples was determined by energy dispersive X-ray fluorescence in equipment Shimadzu EDX720. Thermal analysis was performed using a Shimadzu TGA-50 thermal analyzer, using alumina as reference. The morphology of the samples was investigated by SEM in a microscope Shimadzu SS550 after gold metallization. The textural properties of the samples were characterized using a Micromeritics ASAP-2020 instrument. Profiles of temperature programmed desorption of ammonia, NH_3-TPD, were collected on a Micromeritics Chemsorb 2720.

2.3. Catalytic Reaction. The catalytic dehydration of ethanol was carried out to investigate the influence of the pillarization on the catalytic properties of the lamellar titanoniobates. Catalytic tests were performed in a fixed-bed microreactor containing 100 mg of the catalyst and operated at room pressure, in the range of 250–500°C. Prior to the catalytic activity measurements, the powdered sample was treated in a 30 mL min^{-1} He flow for 1 h. Ethanol was supplied to reactor from a saturator, at 27°C, to provide a 8.6% ethanol/He gaseous mixture in a flow of 30 mL min^{-1}, resulting in a molar flow/weight ratio F/W = 6.34 $mmol\,g^{-1}\,h^{-1}$. Reagents and

Table 1: Elemental analyses of the parent, intercalated, and pillared titanoniobates by EDX.

Sample	K/Ti	Ti/Nb	SiO_2 (%)	Molar composition
KTN	1.00	0.66	—	$K_{0.80}Ti_{0.80}Nb_{1.20}O_5$
HTN	0.08	0.63	—	$K_{0.06}H_{0.72}Ti_{0.78}Nb_{1.22}O_5$
nBTN	0.08	0.63	—	$K_{0.06}(nBuNH_4)_{0.71}Ti_{0.77}Nb_{1.23}O_5$
CTATN	0.05	0.66	—	$K_{0.04}(CTA)_{0.75}Ti_{0.79}Nb_{1.21}O_5$
SiO_2TN	0.05	0.62	18.2	$0.71SiO_2/K_{0.04}H_{0.72}Ti_{0.76}Nb_{1.24}O_5$

products were analyzed online in a Shimadzu GC-17A gas chromatograph equipped with TCD and FID detectors, using an Ellite Plot Q column (30 m × 0,53 mm), using external standards for calibration. Ethanol conversion and ethylene yield were calculated using the following equations:

$$\chi_{\text{ethanol}}\,(\%) = \left(\frac{n_{\text{etOH,in}} - n_{\text{etOH,out}}}{n_{\text{etOH,in}}}\right) \times 100,$$
$$Y_{\text{ethylene}}\,(\%) = \frac{n_{\text{ethylene,formed}}}{n_{\text{etOH,in}}} \times 100, \quad (1)$$

in which χ_{ethanol} is the ethanol conversion; $n_{\text{etOH,in}}$ is the amount of matter of ethanol in the gas feed; $n_{\text{etOH,out}}$ is the amount of matter of ethanol in the reactor outlet; Y_{ethylene} is the ethylene yield; $n_{\text{ethylene,formed}}$ is the amount of matter of ethylene in the reactor outlet.

3. Results and Discussion

The elemental analyses of the samples as determined by EDX are shown in Table 1. The molar composition determined for the as-prepared KTN was $K_{0.80}Ti_{0.80}Nb_{1.20}O_5$, indicating that Ti and Nb have not been incorporated in the same proportion during solid state reaction. The random changes observed in Ti/Nb molar ratios during intercalation and pillaring processes can be attributed to the experimental errors and accuracy of EDX analysis technique. The pillared SiO_2TN sample has presented 18.2% of SiO_2 incorporated in the composite. It is important to mention that H^+, $nBuNH_4{}^+$, and CTA^+ contents in Table 1 are only nominal, because EDX analysis cannot detect H, C, or N in the sample composition.

The X-ray diffraction patterns of the different titanoniobate samples are shown in Figure 1.

The XRD patterns collected for the KTN material are consistent with an orthorhombic perovskite lamellar structure (ICSD number 10491) without indication of contaminant phases. An orthorhombic structure was also assigned to the protonic titanoniobate, $HTiNbO_5$ (ICSD number 31795).

During the cation exchange and pillaring processes, one could observe that the diffraction peak corresponding to d(002) shifts toward lower 2θ values, while diffraction peaks at higher angles decrease in intensity, suggesting that some exfoliation can occur. This is a common feature during pillarization of layered materials, such as clays, hydrotalcites, and layered zeolite precursors [11].

The d(002) reflection is assigned to the basal spacing in the lamellar structure and allows the calculation of the height of the galleries between the lamellae of the titanoniobates,

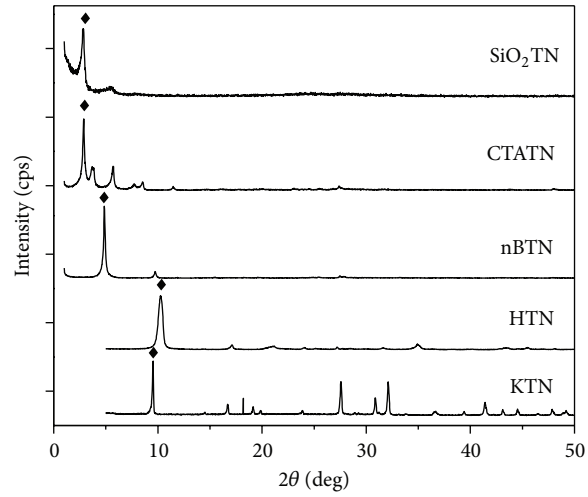

Figure 1: Powder X-ray diffraction patterns for titanoniobates intercalated with different species: K^+ (KTN), H^+ (HTN), n-$BuNH_3{}^+$ (nBTN), CTA^+ (CTATN), and SiO_2-pillared titanoniobate (SiO_2TN). Signal ♦ indicates d(002) reflection.

Table 2: Basal and interlayer spacing for titanoniobates with different interlayer species.

Interlayer species	Basal spacing (Å)	Interlayer spacing (Å)
K^+	9.26	3.16
H^+	8.39	2.29
$ButNH_3{}^+$	18.17	12.07
CTA^+	30.65	24.55
H^+/SiO_2	30.87	24.77

formed by combination of $TiO_6{}^{8-}$ and $NbO_6{}^{7-}$ octahedra. The basal spacing of the samples is shown in Table 2. Taking the thickness of the $TiNbO_5{}^{-6}$ lamella as 6.1 Å [19], the significant increase in the interlamellar spacing is consistent with the size of the species intercalated in the interlayer space of $HTiNbO_5$ [11, 16, 20], as previously described in the preparation Steps 1–3. On the other hand, the slight decrease was assigned to the ionic radii of the exchanged cations, namely, H^+ (0.24 Å) and K^+ (1.51 Å) [21].

The thermal stability of the intercalated materials was investigated and the TG-DTG profiles are collected in Figures 2(a) and 2(b), respectively.

The pristine $K_{0.80}Ti_{0.80}Nb_{1.20}O_5$ (KTN) was very stable up to 1000°C. Thermogravimetric curves for the other materials show a low temperature weight loss at $T < 100$°C,

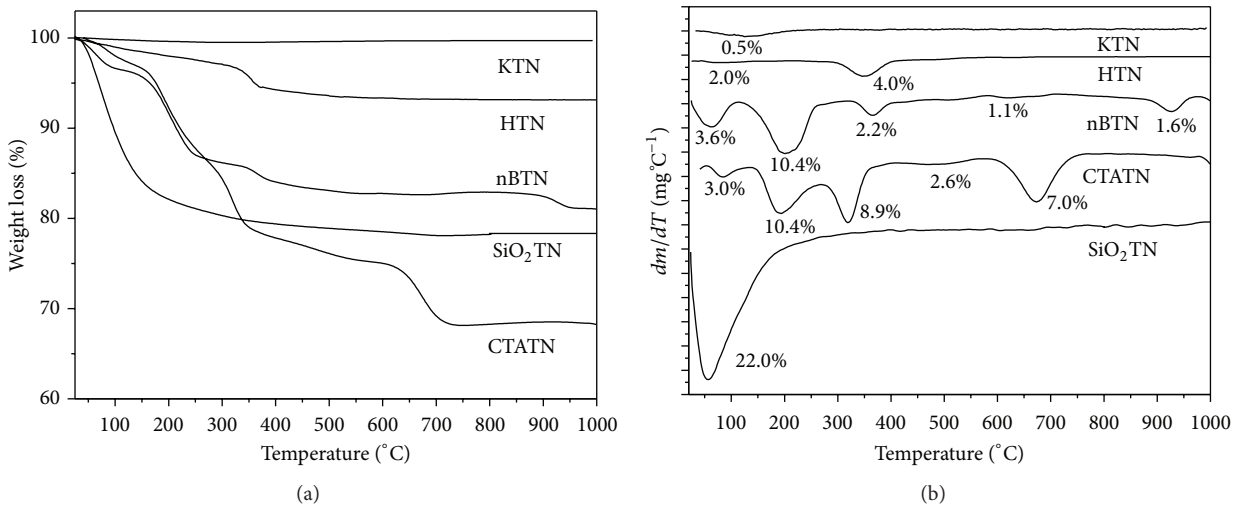

Figure 2: Thermogravimetry (a) and derivative thermogravimetry (b) curves for titanoniobates intercalated with different species: K^+ (KTN), H^+ (HTN), n-$BuNH_3^+$ (nBTN), CTA^+ (CTATN), and SiO_2-pillared titanoniobate (SiO_2TN).

a common feature usually associated with water desorption, and several thermal events at higher temperatures that were assigned to the elimination of either organic molecules (100–300°C) or carbonaceous residues ($T > 450$°C). It was also possible to observe the phase transition from $HTiNbO_5$ to the $Ti_2Nb_2O_9$ tridimensional phase at 347°C [22]. The comparison between weight loss (18.9%) and nominal content of n-$BuNH_3^+$ (18.6%) in the sample nBTN suggested that all H^+ cations reacted during the treatment with n-butylamine. For CTATN sample the total weight loss is lower than the nominal cetyltrimethylammonium content, indicating that n-$BuNH_3^+$ cations were not completely exchanged during the treatment with CTABr. The SiO_2-pillared titanoniobate (SiO_2TN) showed a weight loss of 22% not only due to water in the interlayer space, but also due to dehydroxylation of silica pillars.

SEM micrographs of parent KTN, successively intercalated HTN, BTN, CTATN, and pillared SiO_2TN are shown in Figure 3. $K_{0.80}Ti_{0.80}Nb_{1.20}O_5$ micrograph (KTN, Figure 3(a)) consists of stacking plate-shaped crystallites, very dense, as expected for a material prepared by state solid reaction at high temperature (1150°C). The dimensions of the plates vary in the range of 2 to 5 μm of length and 2 to 4 μm of width.

The shape of the crystallites is better seen in the SEM image of acid sample, HTN (Figure 3(b)), where some exfoliation seems to have occurred. The lamellae have shown an average width of 4 μm.

The SEM image for the sample nBuTN (Figure 3(c)) clearly shows a higher spacing between the rectangular plate-shaped crystallites ($3 \times 5\,\mu$m), suggesting a more efficient exfoliation during the intercalation of n-butylammonium ions. The CTATN sample has shown very well-defined and superposed rectangular crystallites (Figure 3(d)). The plates have varied sizes and a higher degree of exfoliation than n-$BuNH_3^+$ intercalated sample, which is consistent with the length of CTA^+ cation. However, some agglomerates of stacking plates were still observed. The sizes varied from $2 \times 4\,\mu$m to $4 \times 10\,\mu$m.

Table 3: Textural properties determined by N_2 adsorption isotherms using BET and BJH methods for titanoniobates with different interlayer species.

Interlayer species	S_{BET} ($m^2 \cdot g^{-1}$)	V_P ($cm^3 \cdot g^{-1}$)[a]	d_P (nm)[a]
K^+	1.3	0.005	12.0
H^+	13.6	0.027	6.8
H^+/SiO_2	368.4	0.173	14.6

[a]Determined by BJH method.

Pillared sample, SiO_2TN, has presented a high degree of exfoliation (Figure 3(e)); however, some stacking plate-crystallite highly ordered aggregates were still observed, whose size width varied from 2 to 4 μm and length the range from 4 to 10 μm, suggesting that exfoliation is not complete.

The textural properties of the calcined samples are collected in Figure 4 and Table 3.

As expected, a very significant surface area increase was observed for the SiO_2-pillared titanoniobate (SiO_2TN) and surface areas as high as 150 $m^2\,g^{-1}$ have been previously reported for metal oxide-pillared titanoniobates [14, 15].

Nevertheless, the surface area of the SiO_2-pillared titanoniobate obtained after the stepwise intercalation procedure described here was 368 $m^2\,g^{-1}$ and was assigned to a mesoporous structure, consistent with a H4 type hysteresis loop, as shown in Figure 4(c).

The adsorption isotherms of type III collected for the KTN and HTN samples (Figures 4(a) and 4(b)) are assigned to macroporous materials and their surface areas were determined to be 1.4 and 13 $m^2\,g^{-1}$, respectively.

In order to assess the influence of the pillarization procedure on the acid properties of the titanoniobates, NH_3-TPD were carried out for the calcined samples and the results

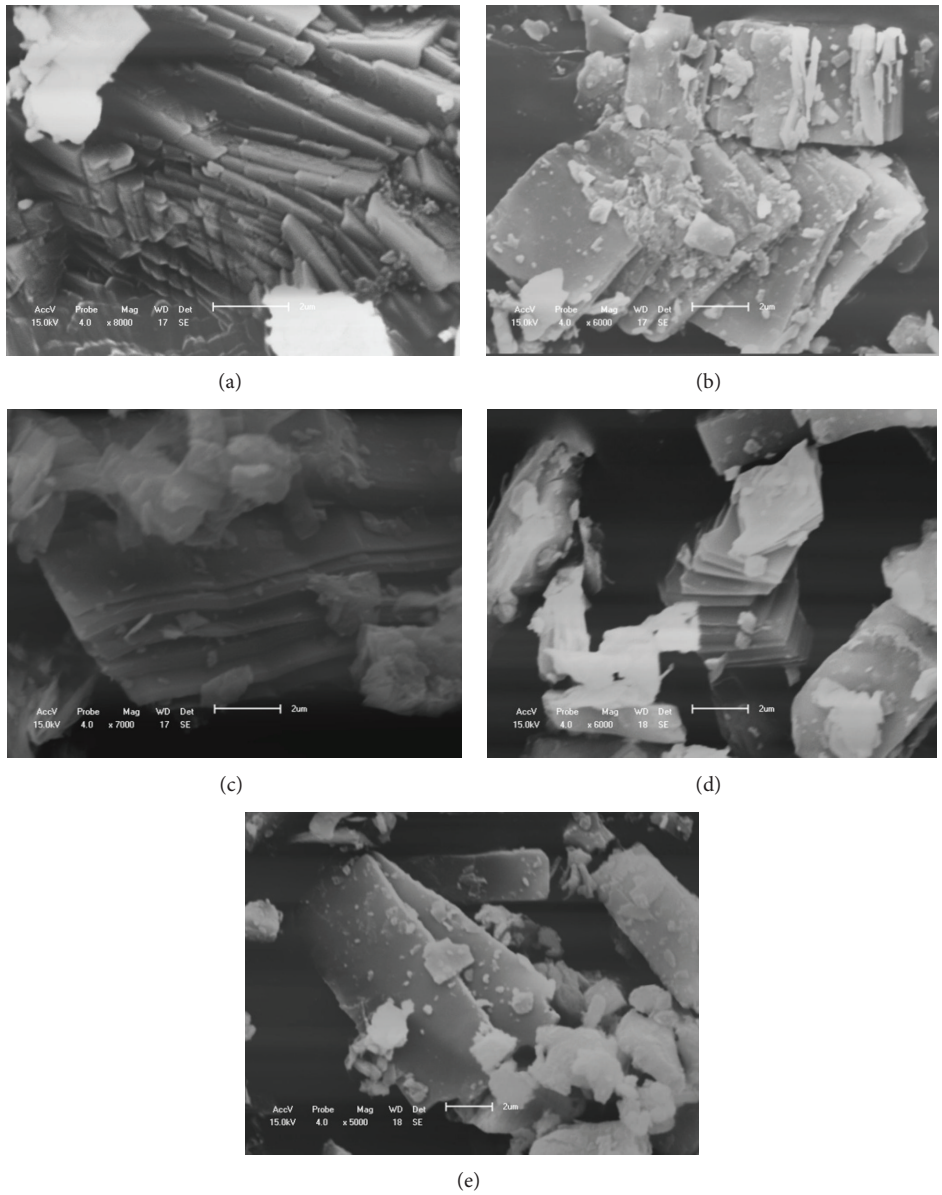

Figure 3: SEM micrographs of layered perovskites intercalated with different species: (a) parent KTN; (b) HTN; (c) nBTN; (d) CTATN, and (e) SiO_2TN.

are shown in Table 4 and Figure 5. All TPD profiles were deconvoluted using Gaussian lines and correlation coefficient $r^2 > 0.99$. For SiO_2TN sample a peak at 156°C for physisorbed has been taken in consideration to warrant a good fitting.

As expected, the pillarization affected the amount and the strength distribution of acid sites. Thus, in spite of the higher amount of acid sites determined for the SiO_2-pillared titanoniobate (SiO_2TN), these sites are distributed in weak (23%), moderate (40%), and strong acid sites (37%). In opposition, the protonic titanoniobate (HTN) showed mainly strong acid sites (63%).

The influence of the textural and chemical modifications due to the pillarization of $K_{0.80}Ti_{0.80}Nb_{1.20}O_5$ (KTN) could be further confirmed on the conversion and product yields plots of the dehydration of ethanol as a function of reaction temperature, as presented in Figure 6.

The dehydration of ethanol is a typical acid-catalyzed reaction and there is a renewed interest on the conversion of bioethanol, a renewable raw material, in order to substitute some important building blocks for the petrochemical industries. For example, the production of the so-called "green polyethylene" using ethylene produced by dehydration of bioethanol has been recently proposed [23, 24] and its technical and economic potential has been discussed in detail [25], emphasizing the role of an active and thermostable catalyst to warrant the viability of the process [26].

Higher ethanol conversions and ethylene yields were achieved in the presence of SiO_2-pillared titanoniobate

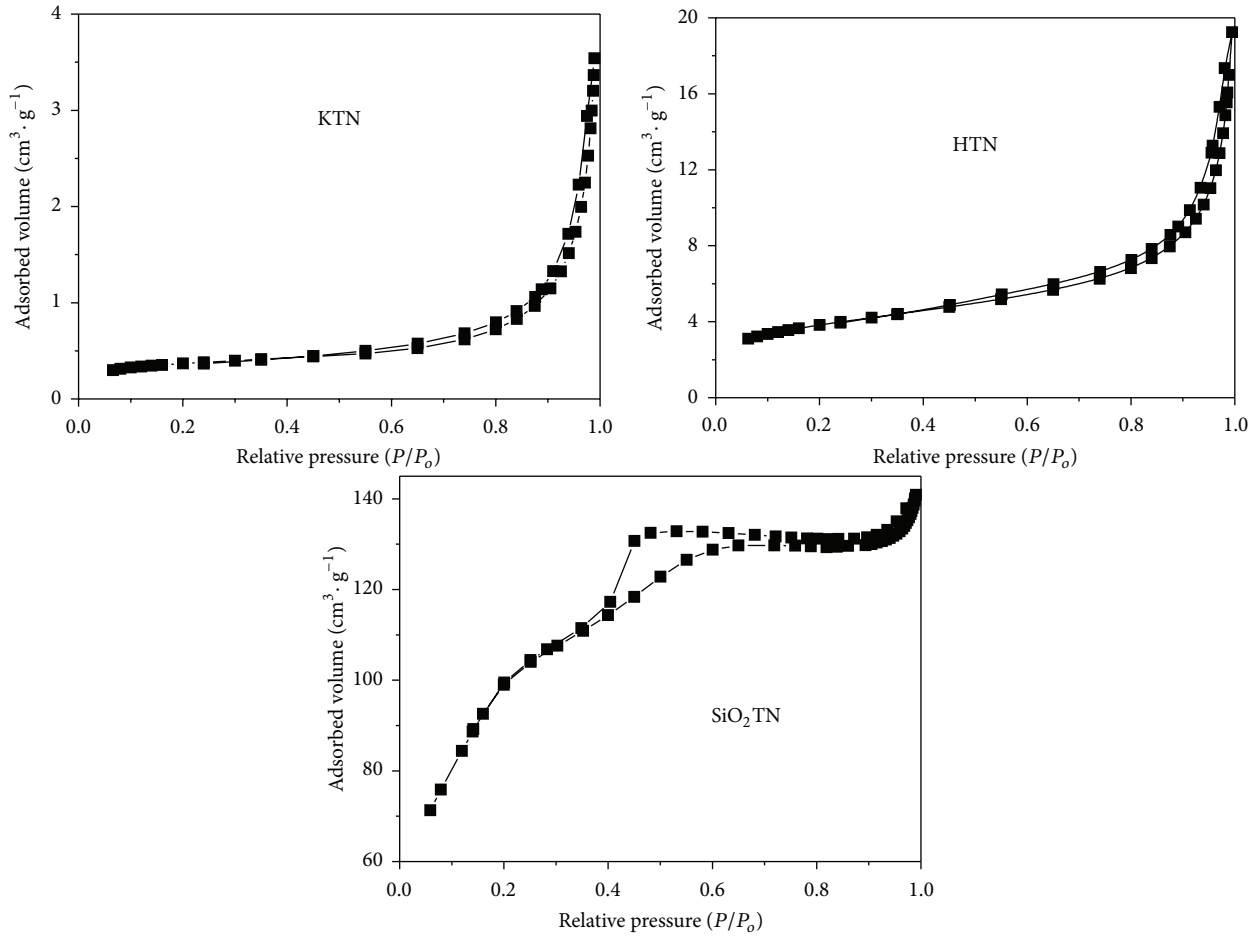

Figure 4: N_2 isotherms for titanoniobates intercalated with different species: K^+ (KTN), H^+ (HTN), and SiO_2-pillared titanoniobate (SiO_2TN).

Table 4: Quantitative analysis and deconvolution of NH_3-TPD profiles.

Sample	Acid strength	T_m (°C)	Density of acid sites (mmol g^{-1})	
			Partial	Total
HTN	Weak	233	0.51 (13%)	3.85
	Moderate	291	0.94 (24%)	
	Strong	407	2.02 (53%)	
		549	0.38 (10%)	
SiO_2TN	Weak	217	0.98 (23%)	4.41
	Moderate	308	1.79 (40%)	
	Strong	457	0.92 (21%)	
		661	0.72 (16%)	

(SiO_2TN), over the investigated temperature range. Ethanol conversion and ethylene yield attained >90% at 350–450°C, corresponding to nearly 100% selectivity toward this product. Ethanol conversion and ethylene yields <30% were achieved in the presence of the protonic titanoniobate (HTN), although selectivity toward ethylene production was >90%, over the investigated temperature range.

These last figures were interpreted as consequence of the much higher surface area and mesoporosity of the SiO_2-pillared titanoniobate (SiO_2TN), allowing a better accessibility of reagents to the inner surface sites than in the protonic titanoniobate (HTN). On the other hand, the high selectivity toward ethylene production achieved in the presence of both protonic and SiO_2-pillared titanoniobates suggested that

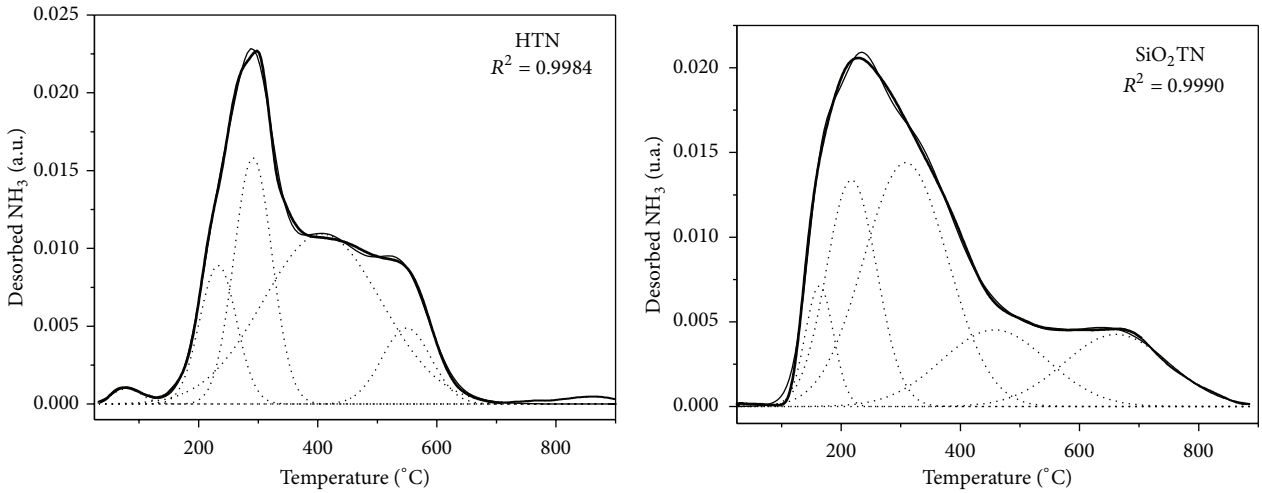

Figure 5: NH_3-TPD profiles for protonic (HTN) and SiO_2-pillared (SiO_2TN) titanoniobates. Experimental profile (—); fitted curve (—); and Gaussian lines used for fitting (···).

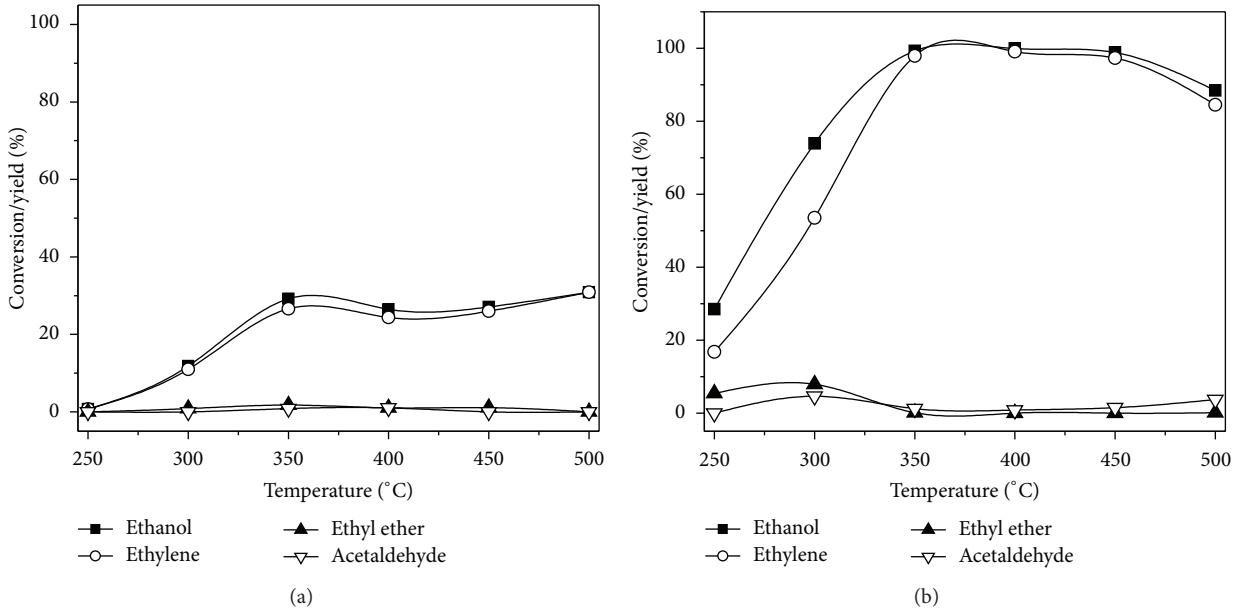

Figure 6: Conversion of ethanol and product yields as a function of temperature during ethanol dehydration on: (a) protonic (HTN) and (b) SiO_2-pillared (SiO_2TN) titanoniobates.

the pillarization procedure affected the amount and strength distribution but did not affect the nature of active acid sites on the lamellar materials.

4. Conclusion

A high surface mesoporous SiO_2-pillared titanoniobate was synthesized from a lamellar perovskite of formula $K_{0.80}Ti_{0.80}Nb_{1.20}O_5$, using a stepwise intercalation procedure. A sequence of n-butylamine, cetyltrimethylammonium bromide (CTABr), and tetraethyl orthosilicate (TEOS) intercalations progressively enlarged the interlayer space, allowing an efficient pillarization. The obtained material showed 368 $m^2\,g^{-1}$ surface area and mesoporosity, in opposition to 1.4 $m^2\,g^{-1}$ and macroporosity of the pristine $K_{0.80}Ti_{0.80}Nb_{1.20}O_5$. The pillarization procedure also affected the amount and strength distribution of acid sites but apparently did not affect the nature of the surface acid sites. These results are consistent with the much higher ethanol conversion and ethylene yields achieved for the catalytic dehydration reaction in the presence of SiO_2-pillared titanoniobate as compared to the protonic titanoniobate.

Conflict of Interests

The authors declare that there is no financial or competing conflict of interests for this work.

Acknowledgment

The authors thank CNPq for the financial support and for the scholarships for M. M. Brito and O. Pergentino.

References

[1] R. A. Schoonheydt, T. Pinnavaia, G. Lagaly, and N. Gangas, "Pillared clays and pillared layered solids," *Pure and Applied Chemistry*, vol. 71, pp. 2367–2371, 1999.

[2] T. J. Pinnavaia, S. D. Landau, M.-S. Tzou, I. D. Johnson, and M. Lipsicas, "Layer cross-linking in pillared clays," *Journal of the American Chemical Society*, vol. 107, no. 24, pp. 7222–7224, 1985.

[3] G. Wallez, D. Bregiroux, K. Popa et al., "$BaAn^{IV}(PO_4)_2$ (AnIV = Th, Np)—a new family of layered double phosphates," *European Journal of Inorganic Chemistry*, no. 1, pp. 110–115, 2011.

[4] S. V. Prasanna and P. V. Kamath, "Synthesis and characterization of arsenate-intercalated layered double hydroxides (LDHs): prospects for arsenic mineralization," *Journal of Colloid and Interface Science*, vol. 331, no. 2, pp. 439–445, 2009.

[5] N. Haydena, J. Diebolda, C. Farrellb, J. Laiblea, and R. Staceyc, "Characterization and removal of DNAPL from sand and clay layered media," *Journal of Contaminant Hydrology*, vol. 86, pp. 53–71, 2006.

[6] W. Hou, Q. Yan, B. Peng, and X. Fu, "Synthesis and characterization of alumina-pillared layered tetratitanates with different interlayer spacings," *Journal of Materials Chemistry*, vol. 5, no. 1, pp. 109–114, 1995.

[7] J. Gopalakrishnan, S. Uma, and V. Bhat, "Synthesis of layered perovskite oxides, $ACa_{2-x}La_xNb_{3-x}Ti_xO_{10}$ (A = K, Rb, Cs), and characterization of new solid acids, $HCa_{2-x}La_xNb_{3-x}Ti_xO_{10}$ ($0 < x \leq 2$), exhibiting variable bronsted acidity," *Chemistry of Materials*, vol. 5, no. 1, pp. 132–136, 1993.

[8] A. D. Wadsley, "Alkali titanoniobates: the crystal structure of $KTiNbO_5$ and KTi_3NbO_9," *Acta Crystallography*, vol. 17, pp. 623–629, 1964.

[9] B. Li, Y. Hakuta, and H. Hayashi, "The synthesis of titanoniobate compound characteristic of various particle morphologies through a novel solvothermal route," *Materials Letters*, vol. 61, no. 18, pp. 3791–3794, 2007.

[10] A. Takagaki, M. Sugisawa, D. Lu et al., "Exfoliated nanosheets as a new strong solid acid catalyst," *Journal of the American Chemical Society*, vol. 125, no. 18, pp. 5479–5485, 2003.

[11] J. He, Q. J. Li, Y. Tang et al., "Characterization of $HNbMoO_6$, $HNbWO_6$ and $HTiNbO_5$ as solid acids and their catalytic properties for esterification reaction," *Applied Catalysis A*, vol. 443-444, pp. 145–152, 2012.

[12] M. Z. Chaleshtori, M. Hosseini, R. Edalatpour, S. M. S. Masud, and R. R. Chianelli, "New porous titanium-niobium oxide for photocatalytic degradation of bromocresol green dye in aqueous solution," *Materials Research Bulletin*, vol. 48, pp. 3961–3967, 2013.

[13] A. S. Dias, S. Lima, D. Carriazo, V. Rives, M. Pillinger, and A. A. Valente, "Exfoliated titanate, niobate and titanoniobate nanosheets as solid acid catalysts for the liquid-phase dehydration of d-xylose into furfural," *Journal of Catalysis*, vol. 244, no. 2, pp. 230–237, 2006.

[14] Y. Chen, W. Hou, C. Guo, Q. Yan, and Y. Chen, "Synthesis and characterization of porous chromia-pillared layered titanoniobate," *Journal of the Chemical Society*, no. 3, pp. 359–362, 1997.

[15] X. Wang, W. Hou, X. Wang, and Q. Yan, "Preparation, characterization and activity of novel silica-pillared layered titanoniobate supported copper catalysts for the direct decomposition of NO," *Applied Catalysis B*, vol. 35, no. 3, pp. 185–193, 2002.

[16] W. Shangguan, K. Inoue, and A. Yoshida, "Synthesis of silica-pillared layered titanium niobium oxide," *Chemical Communications*, no. 7, pp. 779–780, 1998.

[17] X.-J. Guo, W.-H. Hou, S.-M. Liu, and L.-M. Li, "Preparation of TiO_2-pillared $HTiNbO_5$ and catalytic performance in vapor phase beckmann rearrangement reaction of cyclohexanone oxime," *Chemical Journal of Chinese Universities*, vol. 31, no. 6, pp. 1206–1212, 2010.

[18] X. Fan, B. Lin, H. Liu, L. He, Y. Chen, and B. Gao, "Remarkable promotion of photocatalytic hydrogen evolution from water on TiO_2-pillared titanoniobate," *International Journal of Hydrogen Energy*, vol. 38, pp. 832–839, 2013.

[19] J.-F. Lambert, Z. Deng, J.-B. d'Espinose, and J. J. Fripiat, "The intercalation process of N-alkyl amines or ammoniums within the structure of $KTiNbO_5$," *Journal of Colloid and Interface Science*, vol. 132, no. 2, pp. 337–351, 1989.

[20] Y. I. Kim, S. J. Atherton, E. S. Brigham, and T. E. Mallouk, "Sensitized layered metal oxide semiconductor particles for photochemical hydrogen evolution from nonsacrificial electron donors," *Journal of Physical Chemistry*, vol. 97, no. 45, pp. 11802–11810, 1993.

[21] G. L. Miessler, D. A. Tarr, and Inorganic Chemistry Pearson Prentice Hall, New Jersey, NJ, USA, 3rd edition, 2004.

[22] M. Fang, C. H. Kim, and T. E. Mallouk, "Dielectric properties of the lamellar niobates and titanoniobates $AM_2Nb_3O_{10}$ and $ATiNbO_5$ (A = H, K, M = Ca, Pb), and their condensation products $Ca_4Nb_6O_{19}$ and $Ti_2Nb_2O_9$," *Chemistry of Materials*, vol. 11, no. 6, pp. 1519–1525, 1999.

[23] G. Chen, S. Li, F. Jiao, and Q. Yuan, "Catalytic dehydration of bioethanol to ethylene over TiO_2/γ-Al_2O_3 catalysts in microchannel reactors," *Catalysis Today*, vol. 125, no. 1-2, pp. 111–119, 2007.

[24] Y. Guan, Y. Li, R. A. Van Santen, E. J. M. Hensen, and C. Li, "Controlling reaction pathways for alcohol dehydration and dehydrogenation over FeSBA-15 catalysts," *Catalysis Letters*, vol. 117, no. 1-2, pp. 18–24, 2007.

[25] P. Haro, P. Ollero, and F. Trippe, "Technoeconomic assessment of potential processes for bio-ethylene production," *Fuel Processing Technology*, vol. 114, pp. 35–48, 2013.

[26] M. Zhang and Y. Yu, "Dehydration of ethanol to ethylene," *Industrial & Engineering Chemistry Research*, vol. 52, pp. 9505–9514, 2013.